

Magnetic-field effects in ultracold molecular collisions

Alessandro Volpi and John L. Bohn*

JILA and Department of Physics, University of Colorado, Boulder, Colorado 80309

(Received 10 January 2002; published 2 May 2002)

We investigate the collisional stability of magnetically trapped ultracold molecules, taking into account the influence of magnetic fields. We compute elastic and spin-state-changing inelastic rate constants for collisions of the prototype molecule $^{17}\text{O}_2$ with a ^3He buffer gas as a function of the magnetic field and the translational collision energy. We find that spin-state-changing collisions are suppressed by Wigner's threshold laws as long as the asymptotic Zeeman splitting between incident and final states does not exceed the height of the centrifugal barrier in the exit channel. In addition, we propose a useful one-parameter fitting formula that describes the threshold behavior of the inelastic rates as a function of the field and collision energy. Results show a semiquantitative agreement of this formula with the full quantum calculations, and suggest useful applications also to different systems. As an example, we predict the low-energy rate constants relevant to evaporative cooling of molecular oxygen.

DOI: 10.1103/PhysRevA.65.052712

PACS number(s): 34.20.Cf, 34.50.-s, 05.30.Fk

I. INTRODUCTION

The probable success of experiments aimed at producing magnetically trapped ultracold molecular samples depends heavily on the effects of collisional processes. For example, paramagnetic alkali-metal dimers can be produced via photassociation of ultracold atoms [1], but the resulting molecules, typically in high-lying vibrational states, are subject to vibrational quenching collisions [2,3] that can release a large amount of energy and dramatically affect the efficiency of the cooling. Alternatively, cold molecules in their vibrational ground states can be produced either by thermal contact with a cold helium buffer gas [4] or by Stark slowing, for species that possess an electric dipole moment [5,6]. Collisions are of obvious importance to buffer-gas cooling (BGC), as well as to forced evaporative cooling (EC) that will be required to lower the temperature of these gases further and achieve, for instance, Bose-Einstein condensation (BEC). Both processes require large elastic collision rates to thermalize the gas.

So far EC has not been realized in practice for molecules, but the success of the BGC technique for the production of cold CaH [4] and PbO [7] molecules suggests that in the near future it will be possible to achieve BEC using cold molecules. This would open the way for a number of new and fascinating experiments.

In order to be magnetically trapped, atoms or molecules must be in a weak-field-seeking state, i.e., a state whose energy increases with the strength of the magnetic field. For each trappable weak-field-seeking state there is, in general, a lower-energy untrapped strong-field-seeking state, in which the molecules experience a force away from the center of the trap. Collisions can drive transitions between the trapped and untrapped states. These "bad" collisions can cause heating or atom loss. It is, therefore, important to assess the rate constants for the inelastic collisions.

In a series of previous papers the resilience of molecular

oxygen against spin-changing collisions was investigated, in collisions of O_2 molecules both with a helium buffer gas [8], and with other O_2 molecules [9]. These studies found that spin-changing rates due to spin-rotation coupling could be quite large. However, in the case of the $^{17}\text{O}_2$ molecule, where in the limit of zero field the only allowed exit channels are energetically degenerate with the incident channels, spin-flipping transitions require boosting the centrifugal angular momentum from $L=0$ to $L=2$, meaning that these processes are strongly suppressed by the Wigner's threshold laws at collision energies smaller than the height of the exit channel centrifugal barrier.

The results in Refs. [8,9] considered only the case of a vanishing external magnetic field, which is obviously not the case in experiments that trap molecules using spatially inhomogeneous magnetic fields. The present paper, therefore, explores the role that the fields play in determining spin-changing collision rates. As we demonstrate, the presence of a magnetic field causes a Zeeman asymptotic splitting between incident and exit channels, thus lifting the collision energy higher relative to the centrifugal barrier in the exit channel, and removing the Wigner-Law suppression.

Studies of spin-changing ultracold collisions in the presence of an external magnetic field have been performed so far only for atomic species [10–12]. In this paper, we present a detailed dynamical study at cold and ultracold temperatures for the atom-diatom system, $^{17}\text{O}_2\text{-}^3\text{He}$, in a field. The basic model is described in Sec. II. In Sec. III we calculate elastic and inelastic rate constants for collisions involving the lowest-lying trappable state of $^{17}\text{O}_2$ over a wide range of field values (from 0 up to 5000 G), and then discuss the dependence of the rates on collision energy for several representative values of the field. This system is of direct relevance to the BGC of molecular oxygen. Generally, it allows us to quantify the removal of the Wigner's law suppression as the field increases in strength. On this basis we determine a simple one-parameter fitting formula that reproduces the trend with field and energy of the loss rates. In Sec. IV we use this formula to extend previous results on $\text{O}_2\text{-O}_2$ colli-

*Email address: bohn@murphy.colorado.edu

sions to estimate the influence of the field on EC of this system.

II. THEORY

As mentioned in the Introduction, we will consider in this paper molecules consisting of two ^{17}O atoms, whose nuclear spin i is equal to $5/2$. We assume that total nuclear spin $\mathbf{I} = \mathbf{i}_1 + \mathbf{i}_2$ is conserved in the collision and polarized to its maximum value of $\mathbf{I}=5$, implying that the even molecular rotational states N are separated from the odd ones [13]. We limit the discussions of this paper to the “even- N ” manifold of molecular states, which is more appealing for cooling purposes [8,9] having a paramagnetic ground state with spin 1.

The electronic spin \mathbf{S} of the O_2 molecule has magnitude $S=1$ in the electronic ground state $^3\Sigma_g^-$ we are concerned with throughout this paper. The angular momentum \mathbf{S} is coupled to the molecular rotation angular momentum \mathbf{N} to give \mathbf{J} , the total molecular angular momentum, which assumes the values $N-1$, N , and $N+1$ for $N > 0$ and is 1 for $N=0$. The Hamiltonian operator $\hat{\mathbf{H}}_{\text{O}_2}$ for molecular oxygen in the presence of an external magnetic field B can be written as

$$\hat{\mathbf{H}}_{\text{O}_2} = B_e \hat{\mathbf{N}}^2 + \hat{\mathbf{H}}_{fs} + \hat{\mathbf{H}}_B, \quad (1)$$

where B_e is the rotational constant. The $^{17}\text{O}_2$ molecule is considered to be a rigid rotor, with internuclear distance frozen to the equilibrium value of $r_0 = 2.282$ bohr (the rigid rotor model has been shown to be very accurate for this system at the investigated collision energies [14]). The fine-structure Hamiltonian $\hat{\mathbf{H}}_{fs}$ and the Hamiltonian $\hat{\mathbf{H}}_B$ for the interaction of the molecule with the external magnetic field follow the treatment in Ref. [15], disregarding the molecular hyperfine interaction.

The fine-structure Hamiltonian is given as [15]

$$\hat{\mathbf{H}}_{fs} = \left(\frac{2}{3}\right)^{1/2} \lambda T^2(\hat{\mathbf{S}}, \hat{\mathbf{S}}) \cdot T^2(\vec{\alpha}, \vec{\alpha}) + \gamma \hat{\mathbf{N}} \cdot \hat{\mathbf{S}}, \quad (2)$$

where $\vec{\alpha}$ is a unit vector parallel to the molecular axis and T^2 is a second-rank tensor [16,17]. The fine-structure parameters γ and λ have been taken from Ref. [18], where they have been determined by microwave spectroscopy.

The interaction of the field with the electronic spin can be expressed as [19,20]

$$\hat{\mathbf{H}}_B = g \mu_B \hat{\mathbf{S}} \cdot \hat{\mathbf{B}}, \quad (3)$$

where $\hat{\mathbf{B}}$ indicates the external magnetic field, g is the g factor of the electron and μ_B is the Bohr magneton. Following Ref. [20], we ignore a small interaction between the field and the rotational angular momentum.

The matrix elements for $\hat{\mathbf{H}}_{fs}$ and $\hat{\mathbf{H}}_B$ have been given in Ref. [15], Eqs. (A 5) and (A 6), for a Hund’s case b basis set. We note here that the molecular rotational quantum number N is no longer strictly a good quantum number for the molecular states, because different values of N are coupled to-

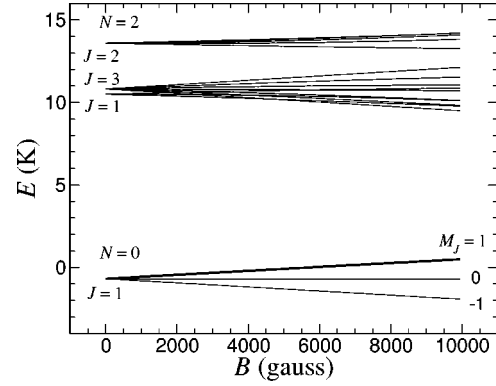


FIG. 1. The lowest-energy Zeeman levels of O_2 for the even- N rotational manifold. These levels are usefully labeled by the approximate rotational (N) and total spin (J) quantum numbers, along with the projection M_J of total spin onto the magnetic field. The heavy line indicates the lowest-lying trappable state $|N J M_J\rangle = |0 1 1\rangle$.

gether by the fine-structure Hamiltonian $\hat{\mathbf{H}}_{fs}$ and by the interaction with the external field. The molecular total angular momentum quantum number J is still a good quantum number with respect to $\hat{\mathbf{H}}_{fs}$, but not with respect to the field interaction $\hat{\mathbf{H}}_B$ term. However, its projection M_J on the laboratory quantization axis is still conserved.

Consequently, our basis functions should be labeled as $|n M_J\rangle$, where n is a shorthand index denoting the pair of quantum numbers (N, J) in the field dressed basis [13]. However, the coupling between different N s is weak (the fine-structure coupling is small compared to the rotational separation) and N can be considered “almost” as a good quantum number. Similarly, J is also approximately good for laboratory-strength magnetic fields, so that we can use without confusion the label $|N J M_J\rangle$.

Magnetic trapping is strongly related to the behavior of the molecules in a magnetic field. The low-energy Zeeman levels of oxygen are displayed in Fig. 1 for the even- N species. (Throughout this paper we report on the energies in units of Kelvin by dividing by the Boltzmann constant k_B . These units are related to wave numbers via $1 \text{ K} = 0.695 \text{ cm}^{-1}$). In order to be trapped in the usual magnetic traps a molecule must be in a weak-field-seeking state, i.e., one whose energy rises with increasing magnetic-field strength. Thus the state $|N J M_J\rangle = |0 1 1\rangle$ is the lowest-lying trappable state of the even- N manifold, and this is the state on which we focus our attention below. This state is indicated by a heavy line in Fig. 1. Higher-lying states with $N \geq 2$ are energetically forbidden at low temperatures.

It is clear from Fig. 1 that for any trapped state there is an untrapped, strong-field-seeking Zeeman state at a lower energy. These states are not merely untrapped but antitrapped, experiencing a force away from the trapping region. In a magnetic trap, collisions with buffer-gas atoms, or more generally with other molecules, will therefore ultimately deplete the trap of its molecular population. The time available for cooling processes like BGC or EC, as well as the lifetime of a molecular Bose-Einstein condensate, is therefore limited

and the knowledge of the rate constants for spin-flipping collisions is essential to predict their feasibility.

In Ref. [8], the theoretical framework for atom-diatom scattering was derived in the limit of zero external field, along the lines of the model originally by Arthurs and Dalgarno [21,22], and properly modified to incorporate the electronic spin of the oxygen molecule. Here, the formulation of the scattering problem is further extended to account for the interaction with the external magnetic field.

The full Hamiltonian operator describing the He-O₂ collision is given by

$$\hat{\mathbf{H}} = -\frac{\hbar^2}{2\mu} \left[\frac{d^2}{dR^2} - \frac{\hat{\mathbf{L}}^2}{R^2} \right] + \hat{\mathbf{H}}_{\text{O}_2} + V(R, \theta), \quad (4)$$

after multiplying the wave function by R in order to remove first derivatives. Here μ is the reduced mass for the He-O₂ system, R is the modulus of the Jacobi vector joining the atom to the molecule's center-of-mass, $\hat{\mathbf{L}}^2$ is the centrifugal angular momentum operator, and $\hat{\mathbf{H}}_{\text{O}_2}$ is the molecular oxygen Hamiltonian defined in Eq. (1). The potential term V , depending on both the Jacobi vector R and on the bending angle θ that the molecule's axis makes with respect to \mathbf{R} , accounts for the He-O₂ interaction. We use the *ab initio* potential energy surface (PES) by Cybulski *et al.* [23], which approximates the true well depth to $\sim 20\%$.

The full multichannel calculation requires casting $V(R, \theta)$ in an appropriate angular momentum basis. Our field dressed basis for close-coupling calculations is then

$$|\text{O}_2(^3\Sigma_g^-)\rangle |\text{He}(^1S)\rangle |N J M_J L M_L \mathcal{M}\rangle, \quad (5)$$

where the electronic spin quantum number S is not explicitly indicated being always equal to 1 in the problem treated here. The quantum number L stands for the partial wave representing the rotation of the molecule and the He atom about their common center of mass, M_L is the projection of $\hat{\mathbf{L}}$ onto the laboratory axis, and \mathcal{M} is the laboratory projection of the total angular momentum, $\mathcal{M} = M_J + M_L$. At the collision energies of interest we assume that the oxygen electronic state and the helium atom state are preserved and, therefore, we suppress the first two kets in Eq. (5) in the following.

We note here that, at variance with the formulation in the zero-field limit, the total angular momentum of the system \mathcal{J} (equal to $\mathbf{N} + \mathbf{S} + \mathbf{L}$) is no longer a good quantum number, because different \mathcal{J} s are coupled together by the interaction with the external field. This means that the dynamical problem is no longer factorizable for different values of \mathcal{J} , thus requiring larger numbers of channels to be treated simultaneously. The problem is still factorizable for \mathcal{M} , but in general, the number of channels to be included for each calculation is much larger than in the previous case. Numerical details of the calculations will be given in the following section.

The coupled-channel equations are then propagated using a log-derivative method [24] and solved subject to scattering boundary conditions to yield a scattering matrix S

$$\langle N J M_J L M_L | S(\mathcal{M}) | N' J' M'_J L' M'_L \rangle. \quad (6)$$

As already noted, the projection of the total angular momentum \mathcal{M} is still a good quantum number, implying that $M_J + M_L = M'_J + M'_L$. Note that, in general, each of the quantum numbers N , J , M_J , L , and M_L are subject to change in a collision, consistent with conserving \mathcal{M} .

Following Ref. [8], the state-to-state cross sections are given by

$$\begin{aligned} \sigma_{N J M_J \rightarrow N' J' M'_J} &= \frac{\pi}{k_{N J M_J}^2} \\ &\times \sum_{L M_L L' M'_L} |\langle N J M_J L M_L | S - I | N' J' M'_J L' M'_L \rangle|^2 \end{aligned} \quad (7)$$

and the corresponding rate coefficients are given by

$$K_{N J M_J \rightarrow N' J' M'_J} = v_{N J M_J} \sigma_{N J M_J \rightarrow N' J' M'_J}, \quad (8)$$

where $v_{N J M_J}$ is the relative velocity of the collision partners before the collision. For notational convenience we will, in the following, refer to collisions that preserve the incident molecular quantum numbers as ‘‘elastic,’’ and those that change the quantum numbers as ‘‘loss.’’

III. RESULTS

In this section we consider elastic and state-changing, inelastic rate constants for the incident channel $|N J M_J\rangle = |0 1 1\rangle$. At the investigated collision energies (from 1 μK up to 10 K) there are two open inelastic channels, namely, $|N J M_J\rangle = |0 1 0\rangle$ and $|0 1 -1\rangle$, both of which are untrapped (see Fig. 1).

A. Magnetic-field dependence

We begin by computing the rate constants for the elastic and spin-flipping transitions $|0 1 1\rangle \rightarrow |0 1 -1\rangle$ and $|0 1 1\rangle \rightarrow |0 1 0\rangle$ in the low-field limit. Results in this section refer to 1- μK collision energy and are converged using partial waves up to $L=6$ and including the rotational states $N=0, 2, 4$, and 6 for the oxygen molecules. The maximum value of R to which the coupled-channel equations are propagated depends on the strength of the field, ranging from 600 bohr in the case of smallest field to 450 bohr for highest values. These parameters assure rate constants convergent within less than 5%, which is adequate for our purposes.

In principle, the scattering matrix should be determined for each possible value of the projection of the total angular momentum \mathcal{M} . However, we know that *s*-wave collisions dominate the incident channel at ultralow collision energies, which corresponds for our incident channel to the value $\mathcal{M}=1$. We have verified that including only the $\mathcal{M}=1$ channels in the calculation changes the results by less than 1% at microkelvin energies; in this section we, therefore, include only this contribution. The number of channels to be propagated according to the given convergent quantum numbers is then only 205.

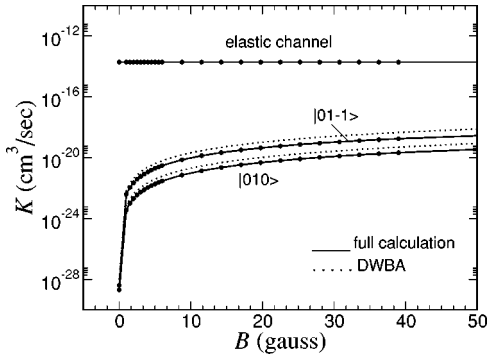


FIG. 2. Rate constants (logarithmic scale) for collisions of ^3He and $^{17}\text{O}_2$ molecules in the $|N J M_J\rangle = |0 1 1\rangle$ initial state as a function of the magnetic field B and collision energy $1 \mu\text{K}$, for low values of the field. Solid lines are the complete quantum mechanical calculation, while dotted lines are the results of the distorted-wave Born approximation (DWBA). For each curve the final state of the oxygen molecule is indicated.

Figure 2 shows elastic and inelastic rate constants at energy $E = 1 \mu\text{K}$ and for low values of the field. The inelastic rate constants are nonzero even at zero field, as shown in Ref. [8]. However, in this limit the final states are degenerate with the initial state, and inelastic transitions are strongly suppressed by the presence of a d -wave centrifugal barrier in the exit channel, whose height is about 0.59 K . This effect is able to suppress the molecule loss, at least as long as the collision energy does not exceed the barrier height [9].

As soon as a field is applied, the thresholds are no longer degenerate in energy, so that the energy in the exit channel is not as far below the centrifugal barrier. As a consequence, inelastic transitions are no longer as strongly suppressed, even in the limit of very low collision energy. Rather, they increase dramatically even in a weak field, with rates being boosted by five or six orders of magnitude in a 1-G field. On the other hand, elastic scattering is nearly unchanged by the field.

This sudden increase of the inelastic transition rates can be reproduced semiquantitatively by applying the distorted-wave Born approximation (DWBA) [22], as has been successfully done for the magnetic dipolar interaction of cold alkali atoms [10,11] as well as in a number of problems in cold collisions [25,26]. The first-order DWBA is a simple two state perturbation approximation applicable in cases where inelastic scattering is weak in comparison with elastic scattering. The DWBA expression for the off-diagonal K -matrix elements is

$$K_{if} = -\pi \int_0^\infty f_i(R) V_{if}(R) f_f(R) dR, \quad (9)$$

where f_i and f_f represent the energy normalized scattering wave function of the initial and final states calculated on the diabatic potential corresponding to the states involved in the inelastic transition. V_{if} is the corresponding diabatic coupling term of the Hamiltonian (4). The first-order DWBA result is shown as a dotted line in Fig. 2.

The DWBA also yields information on the threshold dependence of the loss rates on energy and field. To see this, first note that the spin-changing processes we are considering are strongly dominated at low collision energy by s waves in the incident channel, and by d waves in the exit channel. This change of partial wave is necessary to conserve angular momentum during a collision that changes the molecule's spin. For small values of the magnetic field (for which the Zeeman splitting does not exceed the height of the exit channel centrifugal barrier) the exit channel is still in the threshold regime, whereby the wave functions f_i and f_f in Eq. (9) can be approximated by the small-argument limit of energy-normalized spherical Bessel functions,

$$\begin{aligned} f_i &\propto \sqrt{k_i} j_{L_i}(k_i R) \propto (k_i R)^{L_i+1/2}, \\ f_f &\propto \sqrt{k_f} j_{L_f}(k_f R) \propto (k_f R)^{L_f+1/2}, \end{aligned} \quad (10)$$

where k_i and k_f are the incident and final wave numbers and L_i and L_f are the incident and final partial waves. Assuming a small- R cutoff to insure convergence of the integral in Eq. (9) with respect to $1/R^6$ singularity in the coupling potential $V_{if}(R)$, the energy dependence of the K -matrix element is

$$K_{if} \propto k_i^{L_i+1/2} k_f^{L_f+1/2}. \quad (11)$$

By considering the relationship between K_{if} and the effective rate constant $K_{NJM_J \rightarrow N'J'M'_J}$, it is straightforward to show that the rate constant behaves approximately as

$$K_{NJM_J \rightarrow N'J'M'_J} \propto E^{L_i}(E + \Delta M_J g \mu_0 B)^{L_f+1/2}, \quad (12)$$

where E is the collision energy, and we have taken into account that the final kinetic energy in the exit channel is incremented by an amount $\Delta E_B = \Delta M_J g \mu_0 B$ corresponding to the linear Zeeman shift. $\Delta M_J (= M_J - M'_J)$ stands for the difference between the initial and final values of M_J in the two channels involved in the transition. The actual value of ΔE_B is modified by quadratic Zeeman shift, but the linear approximation is adequate for achieving a simple fitting formula. In the present case, these shifts amount to less than 10% changes in the approximated rate constants. From Eq. (12), considering that in our case $L_i = 0$ and $L_f = 2$, a simple expression for the rate constants can be derived,

$$K_{NJM_J \rightarrow N'J'M'_J} = K_0 \left(\frac{E + \Delta M_J g \mu_0 B}{E_0} \right)^{5/2}, \quad (13)$$

where K_0 represents an overall scaling constant and E_0 is conveniently chosen as the height of the centrifugal barrier in the exit, d -wave channel. In the limit of very low collision energy, the $\Delta M_J g \mu_0 B$ term obviously dominates over E , leading to a nonzero rate constant, as is the case for exothermic collisions.

This simple expression allows us to interpret the threshold behavior of the rates with the field, explaining the $5/2$ exponential dependence on B found in our calculation and shown explicitly in the bilogarithmic plot for the rate constants (Fig. 3). Here the dashed lines represent a fit to the rate constants

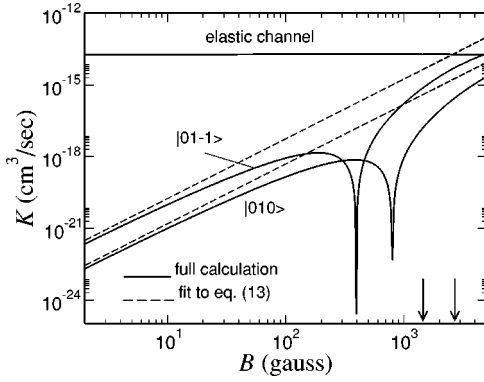


FIG. 3. Rate constants for collisions of ${}^3\text{He}$ and ${}^{17}\text{O}_2$ molecules in the $|N J M_J\rangle = |0 1 1\rangle$ initial state as a function of the magnetic field B and collision energy $1 \mu\text{K}$ (bilogarithmic scale). Solid lines refer to the exact quantum calculation, while dashed lines refer to the fit using Eq. (13). For each curve the final state is indicated. Vertical arrows indicate the values of the field for which the difference of the asymptotic energies $|0 1 1\rangle - |0 1 -1\rangle$ (or $-|0 1 0\rangle$) exceeds the height of the centrifugal barrier.

in the limit of zero magnetic field, yielding coefficients $K_0 = 2.73 \times 10^{-14} \text{ cm}^3 \text{ sec}^{-1}$ and $K_0 = 1.45 \times 10^{-14} \text{ cm}^3 \text{ sec}^{-1}$ for the transition to the final states $|0 1 -1\rangle$ and $|0 1 0\rangle$, respectively. Apart from zeros in the actual rate constants, the overall trend is indeed $K_{N J M_J \rightarrow N' J' M'_J} \propto B^{5/2}$. The zeros in the real rates arise from interferences between the s - and d -wave radial wave functions, as we have verified qualitatively by the DWBA. Nevertheless, the simple one-parameter expression (13) provides a reasonable upper bound to the complete calculation which, it will be recalled, requires a calculation involving 205 coupled channels.

The simple formula (13) holds, of course, only when both incident and final channels are in the threshold regime. Assuming low incident energies, this restriction, therefore, limits the size of magnetic field for which Eq. (13) applies. Namely, this expression is only useful when the Zeeman energy splitting between incident and final states remains smaller than the height of the d -wave centrifugal barrier. For the channels considered here, these fields are 2430 G and 4860 G for the $|0 1 -1\rangle$ and $|0 1 0\rangle$ final states, respectively. Vertical arrows in Fig. 3 indicate these field values. Relation (13) serves as a useful quick fitting formula for data at smaller fields, and allows us to generalize the results obtained in this paper also to different systems. Possible applications are discussed in Sec. IV.

When stronger values of the magnetic field are considered, the DWBA is no longer able to reproduce the full calculation, because the coupling is no longer a weak perturbation. Strong field interaction mixes up different channels leading to a much more complicated picture that cannot be explained in terms of a simple two state model. However, in this limit the loss rate constants seem to be unacceptably large anyway, owing to the effectiveness of spin-rotation coupling in changing spins. For example, For $B \sim 4800 \text{ G}$, the inelastic rate constant for the $|N J M_J\rangle = |0 1 -1\rangle$ exit channel exceeds that for the elastic one. This indicates that in the high field limit fine-structure changing collisions repre-

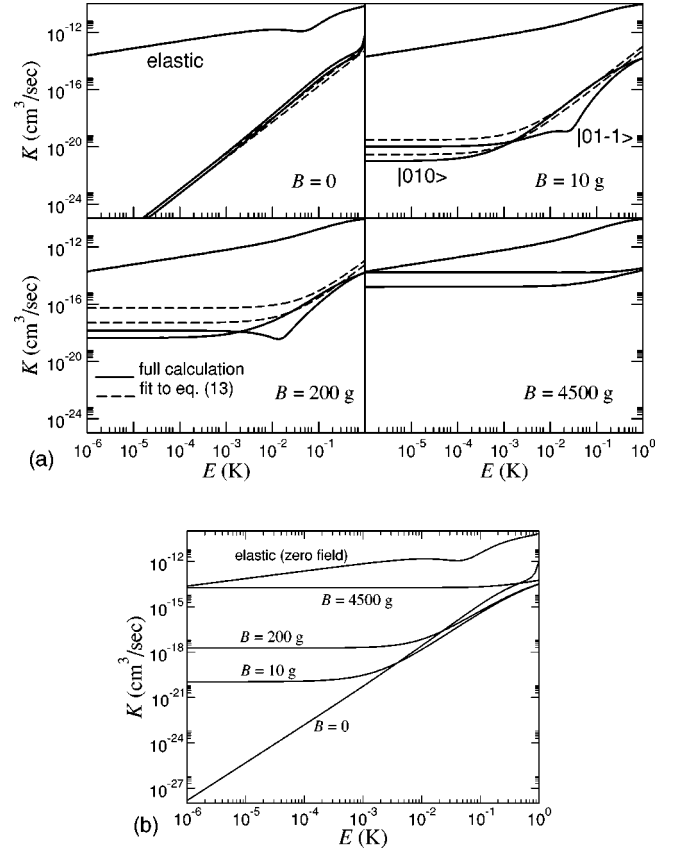


FIG. 4. (a) Collision energy dependence of elastic and inelastic rate constants in the range $1 \mu\text{K} - 1 \text{ K}$ (bilogarithmic scale). In each panel the corresponding value of the magnetic field is indicated. The solid lines refer to the full quantum calculations while dashed lines refer to the inelastic rate constants calculated using relation (13), with values of K_0 as given in the text. (b) shows the total loss rate constant for all four field values simultaneously, to facilitate their comparison. In (b), only the full quantum calculations are shown.

sent a potential limitation for the success of the collisional cooling processes.

B. Collision energy dependence

In this section, the dependence of elastic and inelastic rate constants on the collision energy are analyzed for the zero-field limit and for three representative values of the field, namely, 10, 200, and 4500 G.

In Fig. 4(a), we report our results for collision energies for $1 \mu\text{K} - 1 \text{ K}$ for the four values of the field mentioned above. Elastic scattering, which is largely determined by s waves in both incident and final channels, is weakly affected by the strength of the field. For spin-changing collisions, however, the energy dependence changes dramatically, in accordance with Eq. (13), which is shown in the figure using dashed lines. Again the trends are well represented, although the formula overestimates the rates due to the zeros in the real rates described in the preceding section.

As a general trend, we observe that when the field is increased, the low-energy inelastic rate constants are sub-

stantially pushed up towards the elastic ones, but at higher energies the rates are less sensitive to the field. This is better illustrated in Fig. 4(b), where the total loss rate constants (that is, the sum of the inelastic scattering in the two exothermic channels) for the different values of the field are plotted together with the elastic channel results in zero field (which, as stressed before, are essentially independent of the B value).

In the range of collision energies from 1 μ K to 1 K and for low magnetic fields the rates for elastic collisions remain significantly higher than the rate for the spin flipping. In particular, at buffer-gas-cooling energies of ~ 1 K and below, the inelastic rate constants are in the 10^{-14} cm^3/sec range, and remain so even in the presence of a field. This result verifies the suitability of the $^{17}\text{O}_2$ molecule for BGC. Given the comparatively small uncertainties in the PES [23], the results shown here are probably fairly realistic for the He- O_2 system.

We have continued the analysis in the range of collision energies from 1 to 10 K. We note that for energies larger than the height of the centrifugal barrier, the approximation of including only $\mathcal{M}=1$ in the calculation is no longer accurate within a few percent, as was the case at lower energy. We checked that in this energy range the full calculations including all the possible \mathcal{M} values provides results that differ (in the worst case) by about a factor of 3 for the inelastic channels and by about a factor of 5 for the elastic ones. The full calculation is computationally very expensive for $B>0$, as opposed to the case of zero field where a total- \mathcal{J} basis can be adopted. Results indicate that inelastic rates for high collision energies are not much lower than elastic rates, and of course, become higher still at energies where resonances exist.

At collision energies above 1 K both Feshbach and shape resonances appear in the cross sections, as noted in Ref. [8]. We find that these resonances move somewhat as a function of the magnetic field. Nevertheless, they are sufficiently narrow that they are completely “washed out” by thermal averaging in a gas. We, therefore, present these results as a function of temperature rather than energy. To this end we assume a Maxwellian velocity distribution of the collision partners characterized by a kinetic temperature T . The thermally averaged rate constants are then expressed as

$$\bar{K}(T) = \left(\frac{8k_B T}{\pi \mu} \right)^{1/2} \frac{1}{(k_B T)^2} \int_0^\infty E \sigma(E) e^{-E/k_B T} dE, \quad (14)$$

where k_B is the Boltzmann constant and $\sigma(E)$ stands for cross sections. To compute this average, the values of the cross sections for $E>10$ K are extrapolated from their values at 10 K.

Averaged rate constants are shown in Fig. 5 for the same set of field values as in Fig. 4. The condition for magnetic trapping to be successful is usually expressed as $K_{el} > 10K_{loss}$ [27], so that we can conclude that for collisions of $^{17}\text{O}_2$ with ^3He this condition is fulfilled at least for temperatures up to 1 K and values of the field for which the asymptotic Zeeman splitting does not exceed the height of the exit channel centrifugal barrier.

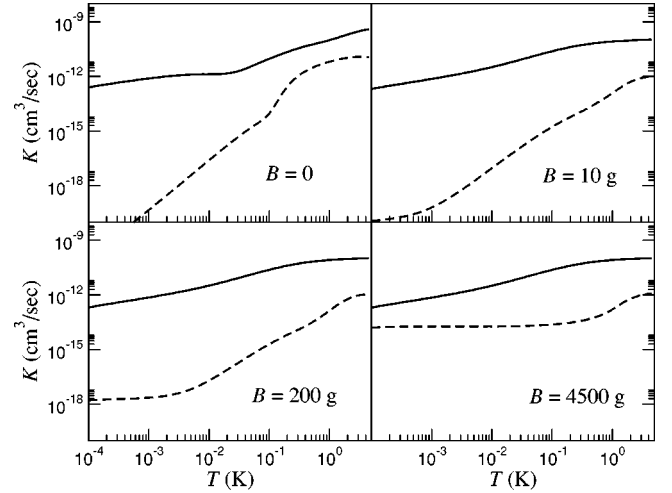


FIG. 5. Thermally averaged elastic (solid line) and total loss (dashed line) rates for $^3\text{He}-^{17}\text{O}_2$ collisions as a function of temperature. In each panel, the corresponding value of the magnetic field is indicated.

IV. APPLICATIONS

Even in the absence of detailed information on cold collisions of a particular molecule, the fitting formula (13) can be used as an approximate guide to what the rates might be. For example, we can inquire about the prospects for evaporatively cooling $^{17}\text{O}_2$ molecules once they have been successfully cooled in a first stage of BGC. For this system, the d -wave centrifugal barrier height is ~ 13 mK, meaning that the threshold law is expected to hold for field values smaller than ~ 53 G for transitions that produce one or more molecules in the $|0 \ 1 \ -1\rangle$ final state.

In the case of $^{17}\text{O}_2$ cold collisions we have access to the zero-field calculations of Ref. [9]. We have fit the energy dependence of all the inelastic rate constants to yield the dashed curve labeled “ $B=0$ ” in Fig. 6, which represents the total loss. The full calculation (solid line) has some additional features due to scattering resonances near zero energy,

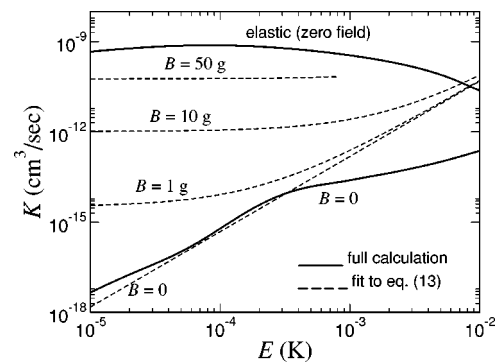


FIG. 6. Comparison between elastic and total loss rate constants for collisions of $^{17}\text{O}_2$ molecules with each other, for several representative values of the field. The zero-field results (solid line) are reproduced from Ref. [9]. The field-dependent estimates (dashed lines) are based on a fit of Eq. (13) to the zero-field rates. Fitted results are shown only for field values and collision energy ranges where Eq. (13) is expected to hold.

but this will not affect our conclusions here. Based on the zero-field fit, we use Eq. (13) to estimate the loss rates in nonzero field. The general trends are the same, namely, the rates rise sharply at low energy, but are roughly field independent at larger energies.

For evaporative cooling to be successful requires, roughly speaking, that the ratio of elastic to inelastic collision rates K_{el}/K_{loss} should exceed 100 [28]. For the estimated results shown in Fig. 6, this condition holds only at energies below ~ 1 mK for fields as low as 10 G, and not at all for near-critical fields of ~ 50 G. Thus evaporative cooling from an initially buffer-gas-cooled sample may prove trickier than previously expected. On the other hand, BGC is characterized by a large number of molecules cooled in the initial step; it is possible that a certain loss can be tolerated, and that a final sample at submicrokelvin temperatures will still hold enough molecules to reach critical phase space density for BEC. Detailed kinetic simulations are required to determine if this is so. Alternatively, a recent proposal suggests that NH molecules could be cooled via Stark slowing to temperatures as low as 1 mK [29]. In this case EC may work quite well.

For many systems of interest to ultracold studies, there does not exist any information on spin-changing collisions at low enough temperatures. In such cases it may be possible to make order-of-magnitude guesses anyway. For example, suppose a rate constant is known for higher-temperature collisions. In the absence of any other information we could simply assert that the rate has the same value at the energy E_0 corresponding to the height of the centrifugal barrier. The fitting formula (13) then gives the behavior of this rate at lower temperatures. For example, the zero-field rate constant in the first panel of Fig. 5 has a value of 10^{-11} cm³/sec at a temperature of 4 K. Extrapolating this value down to $E_0 = 0.59$ K yields a coefficient $K_0 = 7.2 \times 10^{-14}$ cm³/sec for the total loss, higher than the fit to the low-energy calculation just by a factor of 2.

V. CONCLUSIONS

One of the main aims of this paper is to understand in a broad sense collision of paramagnetic molecules in the limit of ultralow temperatures in the presence of a magnetic field. This is a part of our effort in showing that molecules with nonzero spin in the lowest-energy state (such as $^{17}\text{O}_2$ investigated here) can be successfully cooled and used for BEC purposes.

Elastic and inelastic scattering in presence of a magnetic field for the specific system $^3\text{He}-^{17}\text{O}_2$ has been characterized in detail. Our attention has been focused on the lowest-lying trappable state of the molecule. This information is immediately relevant for BGC of molecular oxygen, and suggests that the presence of the field does not particularly hinder the BGC process. This work extends previous predictions that referred to the oxygen molecule in zero field [8,9], and definitely assess the theoretical possibility for trapping this species.

Moreover, we have illustrated the simple underlying physics of spin-changing rates in general. For low enough fields such that both the incident and exit channels are in the threshold regime, the rate constants vary according to the Wigner's-law dependence $(E + \Delta M_J g \mu_0 B)^{5/2}$. This insight allows us to make estimates of rate constants beyond the ones calculated in detail. In particular, a small field was found to have a dramatic effect on the evaporative cooling of $^{17}\text{O}_2$, which must be taken into account in future experiments aimed at quantum degenerate molecular gases.

ACKNOWLEDGMENTS

This work was supported by the National Science Foundation and by NIST. A.V. acknowledges support from the Università degli Studi di Perugia. We acknowledge useful discussions with A. Avdeenkov and J. Hutson.

-
- [1] For recent reviews, see W.C. Stwalley and H. Wang, *J. Mol. Spectrosc.* **195**, 194 (1999); J. Weiner, V.S. Bagnato, S. Zilio, and P.S. Julienne, *Rev. Mod. Phys.* **71**, 1 (1999).
 - [2] N. Balakrishnan, R.C. Forrey, and A. Dalgarno, *Phys. Rev. Lett.* **80**, 3224 (1998).
 - [3] R.C. Forrey, V. Kharchenko, N. Balakrishnan, and A. Dalgarno, *Phys. Rev. A* **59**, 2146 (1999).
 - [4] J.D. Weinstein, R. deCarvalho, T. Guillet, B. Friedrich, and J. M. Doyle, *Nature (London)* **395**, 148 (1998); B. Friedrich, J.D. Weinstein, R. deCarvalho, and J.M. Doyle, *J. Chem. Phys.* **110**, 2376 (1998).
 - [5] H.L. Bethlem, G. Berden, and G. Meijer, *Phys. Rev. Lett.* **83**, 1558 (1999).
 - [6] J.A. Maddi, T.P. Dineen, and H. Gould, *Phys. Rev. A* **60**, 3882 (1999).
 - [7] D. Egorov, J.D. Weinstein, D. Patterson, B. Friedrich, and J.M. Doyle, *Phys. Rev. A* **63**, 30 501 (2001).
 - [8] J.L. Bohn, *Phys. Rev. A* **62**, 32 701 (2000).
 - [9] A.V. Avdeenkov and J.L. Bohn, *Phys. Rev. A* **64**, 52 703 (2001).
 - [10] E. Tiesinga, B.J. Verhaar, and H. T. C. Stoof, *Phys. Rev. A* **47**, 4114 (1993).
 - [11] A.J. Moerdijk and B.J. Verhaar, *Phys. Rev. A* **53**, 19 (1996).
 - [12] H.M.J.M. Boesten, A.J. Moerdijk, and B.J. Verhaar, *Phys. Rev. A* **54**, 29 (1996).
 - [13] M. Mizushima, *The Theory of Rotating Diatomic Molecules* (Wiley, New York, 1975), p. 170.
 - [14] A. Volpi and J.L. Bohn, *Phys. Rev. A* (to be published).
 - [15] R.S. Freund, T.A. Miller, D. De Santis, and A. Lurio, *J. Chem. Phys.* **53**, 2290 (1970).
 - [16] J.H. Van Vleck, *Rev. Mod. Phys.* **23**, 213 (1951).
 - [17] M. Tinkham and M.W.P. Strandberg, *Phys. Rev.* **97**, 937 (1955).
 - [18] G. Cazzoli and C. Degli Esposti, *Chem. Phys. Lett.* **113**, 501 (1985).
 - [19] R.F. Curl, *Mol. Phys.* **9**, 585 (1965).

- [20] A. Carrington, D.H. Levy, and T.A. Miller, *Adv. Chem. Phys.* **18**, 149 (1970).
- [21] A.M. Arthurs and A. Dalgarno, *Proc. R. Soc. London, Ser. A* **256**, 540 (1960).
- [22] M.S. Child, *Molecular Collision Theory* (Dover Publications, Mineola, 1996), p. 100.
- [23] S.M. Cybulski *et al.*, *J. Chem. Phys.* **104**, 7997 (1996).
- [24] B.R. Johnson, *J. Comput. Phys.* **14**, 445 (1973).
- [25] J.L. Bohn and P.S. Julienne, *Phys. Rev. A* **60**, 414 (1999).
- [26] R.C. Forrey, N. Balakrishnan, A. Dalgarno, M.R. Haggerty, and E.J. Heller, *Phys. Rev. A* **64**, 22 706 (2001).
- [27] J.L. Bohn, *Phys. Rev. A* **61**, 40 702 (2000).
- [28] C.R. Monroe, E.A. Cornell, C.A. Sackett, C.J. Myatt, and C.E. Wieman, *Phys. Rev. Lett.* **70**, 414 (1993).
- [29] S.Y.T. van de Meerakker, R.T. Jongma, H.L. Bethlem, and G. Meijer, *Phys. Rev. A* **64**, 41 401 (2001).